Journal of Magnetic Resonance 299 (2019) 21–27

Contents lists available at ScienceDirect

Journal of Magnetic Resonance

journal homepage: www.elsevier.com/locate/jmr

# Increasing nitroxide lifetime in cells to enable in-cell protein structure and dynamics measurements by electron spin resonance spectroscopy

Kevin Singewald, Matthew J. Lawless, Sunil Saxena *

*Department of Chemistry, University of Pittsburgh, Pittsburgh, PA 15260, USA*

ARTICLE INFO

*Article history:*
Received 14 September 2018
Revised 19 November 2018
Accepted 4 December 2018
Available online 6 December 2018

*Keywords:*
ESR
Double electron–electron resonance
In-cell spectroscopy
*Xenopus laevis* oocyte
Nitroxide radicals

ABSTRACT

There is increasing evidence that the stability, structure, dynamics, and function of many proteins differ in cells versus in vitro. The determination of protein structure and dynamics within the native cellular environment may lead to better understanding of protein behavior. Electron spin resonance (ESR) has emerged as a technique that can report on protein structure and dynamics within cells. Nitroxide based spin labels are capable of reporting on protein dynamics, structure, and backbone flexibility but are limited due to nitroxide reduction occurring in cells. In order to overcome this limitation, we used the oxidizing agent potassium ferricyanide ($K_3Fe(CN)_6$) as well as the cleavage resistant spin label 3-malemido-PROXYL (5-MSL). Furthermore, we hypothesized that injection concentration is an important parameter regarding nitroxide reduction kinetics. By increasing the injection concentration of doubly 5-MSL labeled protein into *Xenopus laevis* oocytes, we found an increased nitroxide lifetime. Our work demonstrates unprecedented incubation times of 3-h in-cell and 5-h in-cytosol for double electron–electron resonance (DEER) experiments using nitroxide spin labels. This allows for more meaningful measurements of larger protein systems which may require longer incubation times for equilibration in the cellular milieu. Even longer incubation times are possible by combining our approach with more shielded nitroxides and Q-band.



## 1. Introduction

Electron spin resonance spectroscopy (ESR) in combination with site-directed spin-labeling (SDSL) [1] has proven to be an important tool to understand the structure, flexibility, and backbone dynamics of biomacromolecules. In particular, continuous wave (CW) ESR on nitroxide labeled proteins is able to report on protein secondary structure, solvent accessibility, and backbone mobility [2,3]. Pulsed ESR techniques such as double electron–electron resonance (DEER) [4,5], double quantum coherence (DQC) [6–9], relaxation induced dipolar modulation enhancement (RIDME) [10,11], and single-frequency techniques for refocusing (SIFTER) [12] dipolar couplings have enabled the distance measurement between two paramagnetic tags placed 1.5 to 16 nm apart [4,13]. These ESR techniques help to further elucidate protein structural information that is inaccessible to other methods such as X-ray crystallography and NMR. Most often, these structural measurements are performed in vitro which lacks the crowded environment that a biomacromolecule would be exposed to in its native environment [14,15]. There is growing evidence that function of some proteins may differ in cells versus in vitro. For example, the folding rate and stability of phosphoglycerate kinase increased when introduced to U2OS bone tissue cancer cells and were maximized specifically in the nucleus of the cell [16]. The stability of many proteins also changes due to high molecular crowding [17,18]. Similarly, the cellular environment was shown to prevent a variant of protein L from retaining its globular fold observed in vitro [19]. Often proteins have different enzymatic activity in vivo as well, and these can differ from the measured in vitro activity by over two orders of magnitude [20]. The ability of ESR to report on protein structure and flexibility in-cell makes it an important method to discern these differences between proteins in vivo and in vitro.

Since most proteins do not have intrinsic paramagnetic sites, distance measurements via ESR often rely on site-directed mutagenesis of solvent exposed residues to cysteine. These free thiols allow for the covalent attachment of the methanethiosulfonate spin label (MTSL) to form the R1 sidechain [21–23]. Currently, these MTSL based in-cell distance measurements are limited by the cleavage of the disulfide bond as well as reduction of the nitroxide radical to an ESR inactive hydroxylamine [24–26]. This reduction is primarily due to the presence of antioxidants, such as ascorbic acid and glutathione found in the cellular environment

* Corresponding author.
*E-mail address:* sksaxena@pitt.edu (S. Saxena).

https://doi.org/10.1016/j.jmr.2018.12.005
1090-7807/

[27]. However, reduction of the nitroxide radical is problematic since DEER requires at least two paramagnetic sites to obtain a measurable signal.

Alternative spin-labeling strategies which use reduction-resistant gadolinium (III) [28–30] and triarylmethyl (trityl) radicals [31] have been employed in order to overcome the loss of signal. While both have proven to be useful alternatives, there are limitations. Gadolinium (III) DEER requires higher frequencies, such as W-band (~95 GHz), relative to the nitroxide experiment optimally performed at Q-band (~35 GHz) nowadays and often performed at X-band (~9.5 GHz) as well. Gadolinium binding tags are also larger in size than nitroxide based spin labels, placing the measured spins further away from the protein backbone. Similarly, Trityl radicals show significant promise relative to traditional nitroxide labeling as sterically protected trityl radicals have a longer lifetime in reducing environments [32] as well as longer relaxation times at room temperature [33]. However, many of the trityl labels utilize the reducible disulfide linkage and are also larger relative to typical nitroxide labels.

Despite the progress with alternative spin labels, nitroxide based in-cell measurements remain useful since nitroxides report on backbone flexibility, dynamics, accessibility, in addition to structure. One method used to avoid nitroxide reduction is to freeze the sample immediately after microinjection. Immediate freezing stops all enzymatic processes involved in nitroxide reduction but prevents proteins from diffusing throughout the cell, which limits the biophysical relevance of these measurements. For example, smaller proteins such as GB1 (roughly 6 kDa) injected into *Xenopus laevis* oocytes require ~30 min to reach equilibrium in the cellular milieu [34] while larger proteins may take more time due to their slower diffusional rate.

Therefore, increasing the possible incubation time is of interest. Recently, we showed the nitroxide lifetime in cells could be improved through the use of the oxidizing agent, $K_3Fe(CN)_6$ [34]. This oxidizing agent enables the oxidation of the reduced hydroxylamine back to an ESR-active nitroxide radical. In addition, $K_3Fe(CN)_6$ oxidizes intracellular ascorbic acid, one of the antioxidants involved in nitroxide reduction [35,36]. Currently, only one hour between injection and flash freezing is allowed for reasonable dipolar modulation measurements [37]. An alternative to MTSL is 3-maleimido-PROXYL (5-MSL). 5-MSL overcomes sidechain cleavage by connecting to the protein backbone via a more stable thioether bond rather than the reducible disulfide formed by R1 [37–41]. Hence, loss of nitroxide spin labels due to cleavage of the disulfide bond is prevented. In this paper, we employed both $K_3Fe(CN)_6$ and 5-MSL in order to enhance the allowed incubation time for the purpose of in-cell Double Electron-Electron Resonance (DEER) experiments. We worked to predict the fraction of protein with two unreduced spin labels and studied the lifetime of doubly labeled protein through both DEER and continuous wave time-scan (CW-TS). DEER experiments for oocytes injected with differing concentration of spin labeled protein were explored as well, and we showed that injection concentration effects the allowed incubation time.

## 2. Experimental

### 2.1. Reagents and GB1 expression, purification, and labeling

3-Maleimido-2,2,5,5-tetramethyl−1-pyrrolidinyloxy (5-MSL) nitroxide was obtained from Sigma–Aldrich and dissolved into ethyl alcohol. Potassium ferricyanide, $K_3Fe(CN)_6$, was purchased from Sigma–Aldrich. E15C/K28C GB1 and K28C GB1 expression and purification were performed as previously described [42,43]. The GB1 mutant was reacted with tris(2-carboxyethyl)phosphine (TCEP) overnight at 4 °C to reduce any disulfide formation. To label the protein, GB1 was run through five 5 mL GE Healthcare Hitrap desalting columns, to remove any TCEP, directly into the premade 5-MSL solution such that the final molar ratio was 20:1 5-MSL: GB1. This was allowed to react overnight at 4 °C. The spin labeled protein was concentrated and run through the desalting columns to remove all unreacted label. The final protein solution was in a phosphate buffer (pH 7.75).

### 2.2. Cellular extracts and oocyte microinjection

Healthy *Xenopus laevis* oocytes (stages V–VI) were selected for cytosol preparation and microinjection. They were maintained at 17 °C in a modified Barth's solution (pH 7.60) containing NaCl (88 mM), KCl (1 mM), NaHCO3 (2.4 mM), HEPES (15 mM), Ca (NO3)2 (0.3 mM), CaCl2 (0.41 mM), MgSO4 (0.82 mM), penicillin sodium salt (10 mg/mL), streptomycin sulfate (10 mg/mL), and gentamycin sulfate (100 mg/ml).

To extract the cytosol, oocytes were removed from the Barth's solution and homogenized using a Scilogex D160 tissue homogenizer. Cellular debris was pelleted by ultracentrifugation at 100,000*g* for 30 min at 4 °C using a Beckman Coulter TL-100 ultracentrifuge and cytosol was collected. All cytosol samples were prepared to a total volume of 120 μL, containing a final concentration of 250 μM GB1 and 2.5 mM $K_3Fe(CN)_6$. In the case that no $K_3Fe(CN)_6$ was added, the sample instead contained a comparable volume of phosphate buffer to keep the cytosol volume held constant at 88 μL. Afterwards, 20 μL of glycerol was added as a cryoprotectant.

Microinjections were performed with a Nanoject III microinjector (Drummond Scientific, Broomall, USA) by manually injecting individual oocytes with 50 nL of spin-labeled E15C/K28C GB1 (250 μM or 700 μM) in phosphate buffer containing 2.5 mM or 7 mM $K_3Fe(CN)_6$ respectively at an injection rate of 46 nL/s. Assuming the oocyte was spherical with a 1 mm diameter, the intracellular injected protein concentration is diluted roughly 10-fold. For DEER, 40 oocytes were injected per sample with an injection time of approximately 5 min. The oocytes were washed with MBS to disallow the measurement of possibly leaked protein. Afterwards, the oocytes were individually inserted into a Pyrex sample tube (3 mm I.D. and 4 mm O.D.) and were gently allowed to settle before freezing. For the room temperature in-cell CW, 4 oocytes were injected and were placed along the wall of the Pyrex tube and any excess water along the walls was removed from the sample tube.

### 2.3. ESR measurements

Both continuous wave (CW) and time-scan (CW-TS) in-cytosol experiments were performed on a Bruker ElexSys E580 CW/FT X-band spectrometer using a Bruker ER4122 SHQE-W1 high-resolution resonator. Aliquots were then drawn into Pyrex capillary sample tubes via capillary action. The room temperature (294 ± 1 K) CW experiments were run at a center field of 3500 G with a sweep width of 150 G, a microwave frequency of ~9.87 GHz, a modulation amplitude of 1 G, and a modulation frequency of 100 kHz for a total of 1024 data points using a conversion time of 20.48 ms. CW-TS experiments used the same experimental parameters as CW, except a total of 8192 data points were collected over the course of 5.96 h. The static magnetic field was set 0.3 G to the left of the maximum peak of the nitroxide triplet. The in-cell CW was acquired in an ElexSys E580 CW/FT X-band spectrometer with a Bruker EN4118X-MD5 resonator using the same parameters as the in-cytosol samples.

Four-pulse DEER experiments were performed on a Bruker ElexSys E680 CW/FT X-band spectrometer equipped with a Bruker

EN4118X-MD5 resonator. The cell extract samples (120 μL) consisted of cytosol containing doubly nitroxide-labeled GB1 (250 μM) with 20 μL glycerol and were flash-frozen by immersion in a bath of liquid nitrogen after incubation periods ranging between 0 and 5 h. These experiments were completed at a temperature of 80 K, which was controlled using an Oxford ITC503 temperature controller and an Oxford CF935 dynamic continuous-flow cryostat connected to an Oxford LLT 650 low-loss transfer tube. The experiments done in cells were flash-frozen after incubation periods between 0 and 3 h and DEER experiments were run at either 80 K or 50 K, depending on the incubation time. DEER experiments followed the pulse sequence: $(\pi/2)_{\nu 1}$–$\tau_1$–$(\pi)_{\nu 1}$–t–$(\pi)_{\nu 2}$–$\tau_2$–$(\pi)_{\nu 1}$–$\tau_2$–echo [4]. The observer pulses $(\pi/2)_{\nu 1}$ and $(\pi)_{\nu 1}$ for both in-cytosol and in-cell experiments were 16 and 32 ns, respectively. The pump pulse $(\pi)_{\nu 2}$ was 24 ns and 12 ns for in-cytosol and in-cell experiments respectively. t was increased by a step size of 10 ns for 128 points. The pump frequency $\nu_2$ was placed at the maximum of the echo-detected field-swept nitroxide spectrum and the observer frequency $\nu_1$ was offset downfield by 70 MHz (~25 G). Data acquisition ranged from 3 h to approximately three days. The time domain DEER signal data were analyzed using DeerAnalysis2018 by Tikhonov regularization [44].

CW-TS experiments were all done using the same batch of oocytes in order to keep cytosolic content consistent. Similarly, in-cytosol DEER experiments as well as the CW-TS which served as a comparison to DEER used the same oocyte batch.

## 3. Results and discussion

In order to investigate the feasibility of our in-cell experiments, we employed the use of the immunoglobulin binding domain of protein G (GB1). Cysteine mutations were incorporated into GB1 at an α-helix (E15C) and a β-sheet (K28C) [43] and were subsequently labeled with 3-maleimido-2,2,5,5-tetramethyl-1-pyrrolidinyloxy spin label (5-MSL). These residues were chosen for mutagenesis as they are solvent exposed, allowing for successful spin labeling, and also to serve as a comparison to previous in-cell results using the commonly used methanethiosulfonate spin label (MTSL) [34]. This doubly labeled GB1 mutant enables the measurement of distance constraints via DEER spectroscopy.

Fig. 1 shows how 5-MSL binds to the protein backbone via the formation of a thioether bond which is resistant to cleavage inside a cellular environment [37–41]. However, the enzyme mediated reduction of the nitroxide radical results in an ESR-silent hydroxylamine inside the cell. The hydroxylamine was shown to be further reduced to a secondary amine in human keratinocyte cells [45]. In addition to reduction, the loss of nitroxide signal is possible by other means, such as oxidation or dimerization. In the cell, reduction is the main pathway of nitroxide metabolism [46]. The addition of the oxidizing agent potassium ferricyanide, $K_3Fe(CN)_6$, promotes a back-reaction converting the hydroxylamine back to a nitroxide radical [34,35]. Here, we seek to employ 5-MSL in conjunction with $K_3Fe(CN)_6$ to extend the lifetime of the nitroxide sidechain inside the cellular environment. The cells remained healthy upon injecting 3.5 mM $K_3Fe(CN)_6$ for at least 18 h, indicating this injection does substantially affect the viability of the oocyte (Fig. S5). This approach would therefore be of value for substantial biophysical research, such as the effect of cellular crowding on structure, dynamics, and protein-protein interactions. However, the use of this agent may be problematic when probing events including physiological redox processes.

*Continuous wave time-scan in cytosol extract:* To confirm that the addition of the oxidizing agent $K_3Fe(CN)_6$ is a viable method of extending the lifetime of nitroxide radicals in cells, we performed continuous wave time-scan (CW-TS) experiments. Since the line shape of the continuous wave (CW) spectrum does not change (Fig. S1), the CW-TS intensity is proportional to the spin concentration. The intensity decay at a constant magnetic field on the CW spectrum, shown in the inset of Fig. 2, is directly related to the reduction kinetics of our ESR-active nitroxide. Fig. 2 shows the

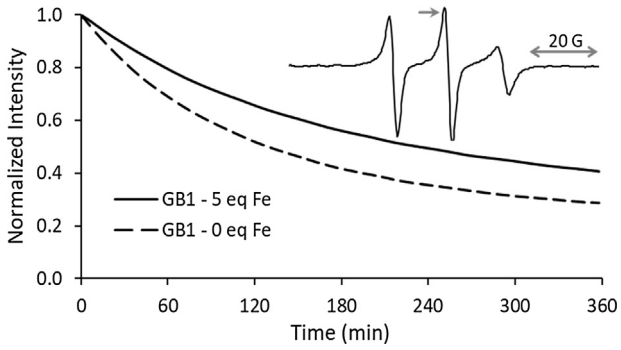


**Fig. 2.** CW-TS of doubly labeled GB1 incubated in cytosol extract with both the addition of 0 (dashed) and 5 (solid) molar equivalence of $K_3Fe(CN)_6$. Inset: The room temperature CW spectrum of 5-MSL labeled GB1 in cytosol. The gray arrow points to the magnetic field used in the time-scan experiments.

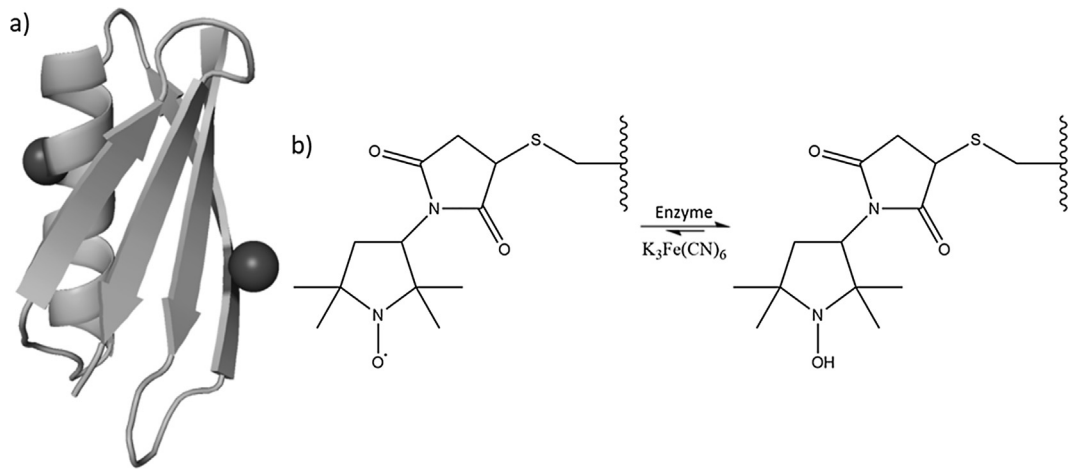


**Fig. 1.** (a) The immunoglobulin binding domain of protein G, GB1, (PDB ID: 5BMG). GB1 was doubly labeled with 5-MSL at residues 15 and 28 on the β-sheet and α-helix respectively (black spheres). b) 5-MSL connects to the protein backbone through the formation of an irreducible thioether bond. The enzyme mediated reduction of the nitroxide can be combated with the addition of the oxidizing agent $K_3Fe(CN)_6$.

results of the CW-TS experiments, which were run in the cytosol extract of *Xenopus laevis* oocytes using 250 μM E15C/K28C GB1 (500 μM of the spin label) with and without the addition of 5 M equivalence [34] of $K_3Fe(CN)_6$ (2.5 mM). CW-TS of 500 μM free 3-carboxy-PROXYL (PCA) [34] and 5-MSL without $K_3Fe(CN)_6$ are also shown in Fig. S2. The CW-TS clearly indicates that the reduction of the nitroxide contained by the 5-MSL labeled GB1 is slowed by the presence of $K_3Fe(CN)_6$. Assuming pseudo first order kinetics, the rate constant decreased by roughly 32%, from $0.534 \pm 0.001\ h^{-1}$ to $0.364 \pm 0.001\ h^{-1}$ after the addition of $K_3Fe(CN)_6$. These rate constants assume that the reduction of the two labeled residues on the α-helix and β-sheet follow similar kinetics, as they are both solvent exposed sites. These rate constants also assume pseudo-first order kinetics despite the multiple cellular processes involved in nitroxide metabolism. This decrease is most likely due to two factors. Firstly, the $K_3Fe(CN)_6$ promotes a back reaction with the reduced hydroxylamine as well as reacting with antioxidants within the cell [35,36]. These results confirm that the addition of an oxidizing agent substantially elongates the lifetime of the bound 5-MSL nitroxide radical.

Because the ultimate goal is to determine structural constraints by obtaining distance measurements between two spin labels, we analyzed the CW-TS data to estimate the doubly and singly labeled protein concentration as a function of incubation time. Again, under the assumption that the 5-MSL attached to the α-helix and β-sheet will follow similar reduction kinetics, the fraction of doubly, singly, and unlabeled labeled protein is estimated as follows:

$$f_2(t) = I(t)^2 \tag{1a}$$

$$f_1(t) = 2I(t)[1 - I(t)] \tag{1b}$$

$$f_0(t) = [1 - I(t)]^2 \tag{1c}$$

where t is the incubation time, $f_n(t)$ is the fraction of protein with n paramagnetic sidechains, and I(t) is the relative CW intensity at time t normalized to unity at t = 0. The intensity of the CW-TS is directly proportional to the number of an ESR active species. The normalized CW-TS intensity, I(t), is therefore equivalent to the probability of finding a labeled residue which remained paramagnetic. Similarly, $1 - I(t)$ is the probability that residue is was reduced to a hydroxylamine. It follows that the fraction of doubly labeled species is $I(t)^2$; the fraction of completely silent species is $[1 - I(t)]^2$; and fraction of singly reduced species is $I(t) * [1 - I(t)] + [1 - I(t)] * I(t)$. Fig. 3 shows the contribution of doubly and singly labeled protein at each time point of the CW-TS. For the purposes of ESR, unlabeled protein does not contribute to the detected signal and therefore we only consider the relative percentages of doubly and singly labeled protein using:

$$f_2'(t) = \frac{f_2(t)}{f_1(t) + f_2(t)} \tag{2}$$

where $f_2'(t)$ is the fraction of doubly labeled protein relative to only ESR active species. From these predictions, the percentage of doubly labeled protein in cytosol extract should be 19% after 6 h of incubation.

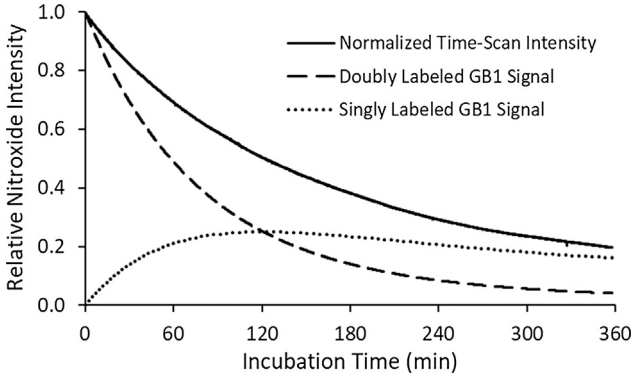


**Fig. 3.** CW-TS experiment fit by the addition of the doubly (dashed) and singly (dotted) labeled protein. Note that the CW-TS above is different than showed in Fig. 2. This experiment was done with the same cytosol batch used in DEER experiments discussed later while data discussed in Fig. 2 used a separate cytosol batch.

*DEER measurements in cytosol:* Having confirmed that $K_3Fe(CN)_6$ slows down nitroxide reduction, we performed DEER measurements on 5-MSL labeled E15C/K28C GB1 in cytosol. Fig. 4a shows the background subtracted time domain DEER of the 5-MSL labeled E15C/K28C GB1 at various incubation times, or the time between introducing GB1 to the cytosol extract and flash-freezing to stop any further enzymatic activity. Note that due to the time required to prepare samples, a zero-minute incubation is unfeasible and therefore the minimum incubation time was ~1 min for the in-cytosol experiments. Measurable modulations were achieved after 5 h of incubation. The overlaid distance distributions, shown in Fig. S3, show that distributions between in vitro and in-cytosol samples were consistent up to 4 h of incubation. The small deviation observed for the 5-h sample may be due to the lower signal to noise ratio of the DEER signal.

*DEER measurements in-cell:* Additionally, we acquired DEER measurements of 5-MSL labeled GB1 injected into stage V-VI *Xenopus laevis* oocytes. Originally, in-cell experiments were done with GB1 injection concentrations of 250 μM to serve as a comparison to previously published data on R1 labeled GB1 [34] as shown in Fig. 5a. We were able to obtain reasonable modulation depths of 5% after a 2-h incubation. We hypothesized that injecting a higher concentration of GB1 would result in one of two outcomes. Either there is a faster rate of reduction due to the increased concentration of protein or the intracellular antioxidants would become limiting and allow for longer incubation times. As such, we acquired DEER of oocytes injected with 700 μM GB1. Fig. 5b shows a modulation depth of 5% after an unprecedented 3 h. In the past, measurable dipolar modulations in *Xenopus laevis* oocytes were successfully obtained only after 60 min for 5-MSL labeled ubiquitin [37] and 30 min for R1 labeled GB1 [34]. We believe that the three-hour incubation was possible due to the ascorbic acid being limited relative to the nitroxide concentration. Distance distributions for the in-cell experiments are shown in Fig. S3 which shows most probable distances averaging around 2.78 nm.

We note incubation times longer than 3 h are likely possible through the combination of $K_3Fe(CN)_6$ with the sterically protected nitroxide spin label, M-TETPO [41]. In the M-TETPO label the nitroxide radical is shielded by changing the *gem*-dimethyl used in 5-MSL to *gem*-diethyl group. Similarly, the use of higher sensitivity Q-band experiments may allow for data acquisition at longer incubation times.

*Fraction of doubly labeled protein:* Finally, the fraction of doubly labeled protein for all the DEER experiments were calculated and are shown in Fig. 6a. These were calculated by using the modulation depth, λ, of the DEER time domain signal as it contains information about the fraction of doubly labeled protein given by [47,48]:

$$\lambda = 1 - \sum_{n=1}^{n_{max}} f_n (1 - p_b)^{n-1} \tag{3a}$$

where $p_b$ is the probability of exciting a b-spin, n is the number of paramagnetic sites present in each species, and $f_n$ is the fraction of ESR-active species with n spins. For the case in which there is at

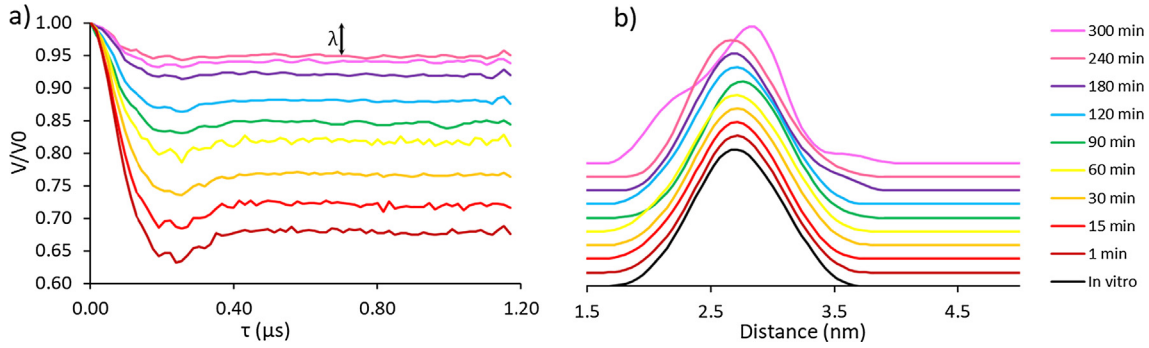


**Fig. 4.** The in-cytosol (a) background subtracted time domain DEER signal and (b) distance distribution of 5-MSL labeled E15C/K28C GB1 after incubation times ranging from 1 to 300 min. The modulation depth λ is defined by the difference between the maximum and the value at which the signal reaches a baseline, as shown for the 300 min incubation in cytosol.

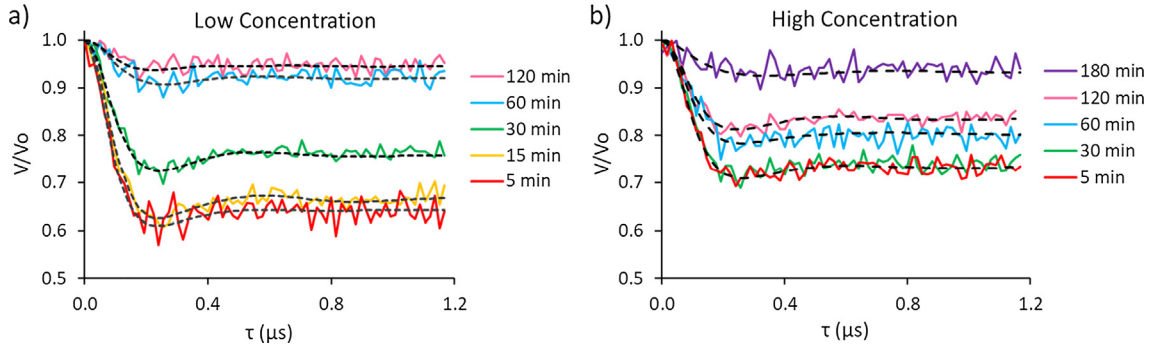


**Fig. 5.** Background subtracted time domain DEER signal of 5-MSL labeled E15C/K28C GB1 after incubation in *Xenopus laevis oocytes* at injection concentrations of (a) 250 μM and (b) 700 μM 5-MSL labeled GB1. Measurable modulations were obtained up to two hours at lower injection concentrations and 3 h at a higher injection concentration.

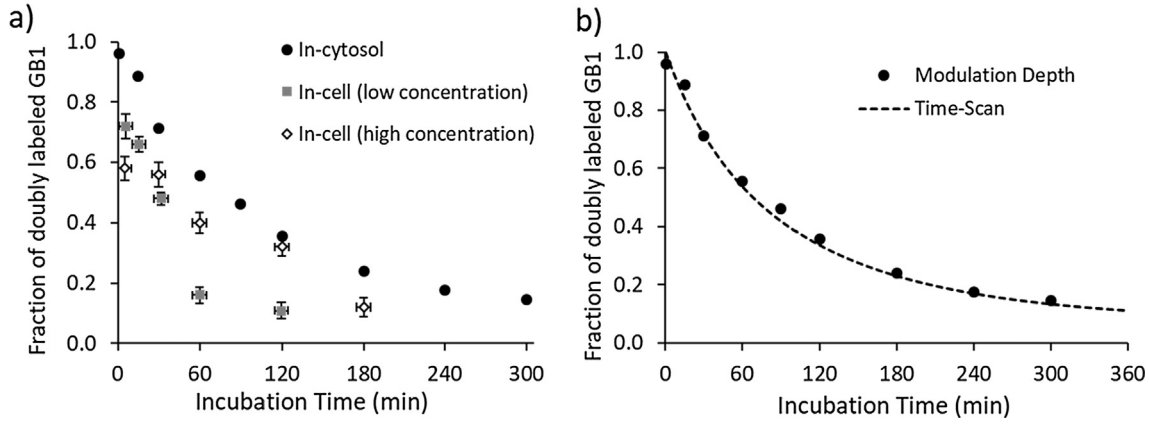


**Fig. 6.** (a) The fraction of doubly labeled protein predicted from DEER for the in-cytosol (black circles) and in-cell at a low (gray squares) and high (white diamonds) injection concentration. The errors in incubation time for the in-cell experiments are due to the time required to inject the oocytes. (b) The fraction of doubly labeled GB1 in cytosol calculated from both the CW-TS (dashed line) and DEER modulation depths (black circles). They follow the same trend implying that sidechain cleavage does not occur.

most 2 spins per system, such as our doubly labeled GB1, Eq. (3a) simplifies to:

$$\lambda = f_2 p_b \tag{3b}$$

From these equations, it is evident that the reduction of doubly labeled to singly labeled protein decreases the experimental modulation depth and our work to increase the lifetime of 5-MSL in turn increased the possible incubation time.

For experiments done in cytosol, a pump pulse of 24 ns was used and $p_b$ was calculated to be 0.32 [49]. Therefore, the in-cytosol results have a calculated modulation depth of 32% if the protein was fully labeled which is in strong agreement with the 31% modulation depth for the 1 min incubation as shown in Fig. 4a. This result implies that no significant reduction occurred between the time taken to prepare the sample. We were able to obtain measurable modulations after an incubation of 5 h. This time could feasibly be further extended by increasing $p_b$ via a shorter pump pulse, and the use of shielded nitroxides.

For experiments done in cells, a pump pulse of 12 ns resulted in a calculated $p_b$ of 0.50. Compared to the in-cytosol experiments shown in Fig. 4, the initial loss of modulation depth was noticeably faster in cells. likely due to membrane associated factors such as thioredoxin [50] and glutathione reductase [51]. Over 20% of GB1 underwent reduction after 5 min in cells at a lower injection

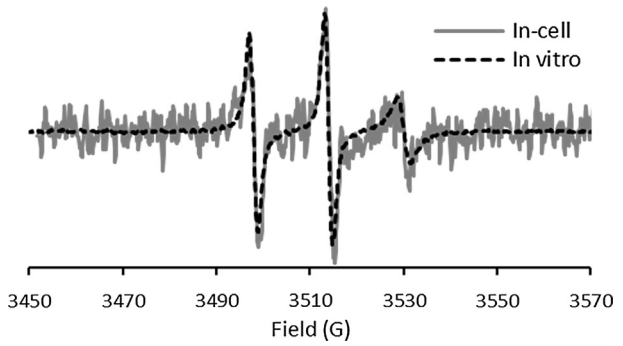


**Fig. 7.** Room temperature CW spectrum in vitro (black dashed) and in Xenopus laevis oocytes (gray solid). Both spectra have a similar line shape and therefore shows no measurable difference for the in-cell and in vitro dynamics of the GB1 α-helix. Note that the two spectra were acquired at different microwave frequencies, as such we shifted the in-cell spectrum to be overlaid with the in vitro data.

concentration while over 40% at the higher concentration. Regardless, the fraction of doubly labeled protein after 3 h was 12 ± 3% which is similar to the 11 ± 3% of doubly labeled GB1 after only 2 h at a lower injection concentration. This emphasizes the importance of injection concentration as a parameter for in-cell DEER.

In order to discern whether 5-MSL cleavage has occurred, we overlaid the calculated fraction of doubly labeled protein calculated from the in-cytosol DEER and CW-TS experiments using equation 2 (cf. Fig. 6b). In the case that sidechain cleavage occurred, this would result in two individual species that are both ESR active, compared to nitroxide reduction which results in one. Since DEER is sensitive to the number of spins per system and CW-TS only detects the total number of spins, we would expect a lower predicted fraction of doubly labeled protein from DEER. Fig. 6b shows the comparison between the fraction of doubly labeled GB1 predicted by both the CW-TS and DEER experiments. The consistency between these two experiments implies that 5-MSL cleavage is minimal in the cellular environment.

*Room temperature continuous wave spectrum in-cell:* One important use of nitroxide based spin labels over some alternatives is the ability of nitroxides to report on in-cell protein dynamics via room temperature CW-ESR experiments [39,52]. As such, we labeled K28C GB1 with 5-MSL and acquired CW spectra at room temperature, both in vitro and in-cell, as shown in Fig. 7. The in-cell CW was acquired after allowing a ~30-min incubation of the 5-MSL labeled K28C GB1 to allow for the protein to equilibrate. Because of the similar line shape between the two spectra, we cannot confidently identify a difference in dynamics between the in vitro and in-cell dynamics for this site α-helical site in GB1.

## 4. Conclusion

Here we have shown that the combination of $K_3Fe(CN)_6$ with a higher injection concentration extends the time of incubation allowed for ESR measurements. First, we showed that 5 M equivalence of $K_3Fe(CN)_6$ to protein bound 5-MSL slows its reduction kinetics by 32%. For use in DEER, labeling GB1 with 5-MSL over the commonly used R1 sidechain extended the feasible in-cell incubation time from 30 min to 2 h under the same conditions. Following a 2.8-fold increase in GB1 concentration, DEER measurements were obtained after an incubation of 3 h in cells. Finally, we showed that the combination of $K_3Fe(CN)_6$ and 5-MSL allowed for a 5-h incubation in cytosol. Although smaller proteins such as GB1 only need 30 min to diffuse throughout the oocyte, this increase in allowed incubation time enables the meaningful analysis of larger proteins as, for example, the diffusion coefficient is halved for a protein double the size. Similarly, smaller proteins can be more easily analyzed after shorter incubation periods due to the deeper modulation depths. Therefore, by optimizing injection concentration as well as introducing an oxidizing agent, ESR will become a more viable method to study biomacromolecules inside their native cellular environment. Even longer incubation times could be achievable through the use of Q-band or by combining these methods with the sterically shielded M-TETPO spin label [41].

## Acknowledgments

This work was supported by the National Science Foundation (NSF MCB-1613007). The spectrometer was funded by the National Science Foundation (NSF MRI-1725678). We would like to thank Dr. Shaohu Sheng for supplying the oocytes used in our experiments. All work done regarding the oocyte extraction was supported by the Pittsburgh Center for Kidney Research (P30 DK079307).

## Appendix A. Supplementary material

Supplementary data associated with this article can be found, in the online version, at https://doi.org/10.1016/j.jmr.2018.12.005.

## References

[1] W.L. Hubbell, C.J. López, C. Altenbach, Z. Yang, Technological advances in site-directed spin labeling of proteins, Curr. Opin. Struct. Biol. 23 (2013) 725–733.
[2] W.L. Hubbell, H.S. McHaourab, C. Altenbach, M.A. Lietzow, Watching proteins move using site-directed spin labeling, Structure 4 (1996) 779–783.
[3] W.L. Hubbell, C. Altenbach, Investigation of structure and dynamics in membrane proteins using site-directed spin labeling, Curr. Opin. Struct. Biol. 4 (1994) 566–573.
[4] M. Pannier, S. Veit, A. Godt, G. Jeschke, H.W. Spiess, Dead-time free measurement of dipole-dipole interactions between electron spins, J. Magn. Reson. 142 (2000) 331–340.
[5] A.D. Milov, A.B. Ponomarev, Y.D. Tsvetkov, Electron-electron double resonance in electron spin echo: model biradical systems and the sensitized photolysis of decalin, Chem. Phys. Lett. 110 (1984) 67–72.
[6] S. Saxena, J.H. Freed, Double quantum two-dimensional Fourier transform electron spin resonance: distance measurements, Chem. Phys. Lett. 251 (1996) 102–110.
[7] P.P. Borbat, J.H. Freed, Multiple-quantum ESR and distance measurements, Chem. Phys. Lett. 313 (1999) 145–154.
[8] M. Bonora, J. Becker, S. Saxena, Suppression of electron spin-echo envelope modulation peaks in double quantum coherence electron spin resonance, J. Magn. Reson. 170 (2004) 278–283.
[9] P.P. Borbat, A.J. Costa-Filho, K.A. Earle, J.K. Moscicki, J.H. Freed, Electron spin resonance in studies of membranes and proteins, Science 291 (2001) 266.
[10] S. Milikisyants, F. Scarpelli, M.G. Finiguerra, M. Ubbink, M. Huber, A pulsed EPR method to determine distances between paramagnetic centers with strong spectral anisotropy and radicals: the dead-time free RIDME sequence, J. Magn. Reson. 201 (2009) 48–56.
[11] L.V. Kulik, S.A. Dzuba, I.A. Grigoryev, Y.D. Tsvetkov, Electron dipole–dipole interaction in ESEEM of nitroxide biradicals, Chem. Phys. Lett. 343 (2001) 315–324.
[12] G. Jeschke, M. Pannier, A. Godt, H.W. Spiess, Dipolar spectroscopy and spin alignment in electron paramagnetic resonance, Chem. Phys. Lett. 331 (2000) 243–252.
[13] T. Schmidt, M.A. Wälti, J.L. Baber, E.J. Hustedt, G.M. Clore, Long distance measurements up to 160 Å in the GroEL tetradecamer using Q-band DEER EPR spectroscopy, Angew. Chem. Int. Ed. 55 (2016) 15905–15909.
[14] S.B. Zimmerman, S.O. Trach, Estimation of macromolecule concentrations and excluded volume effects for the cytoplasm of Escherichia coli, J. Mol. Biol. 222 (1991) 599–620.
[15] C.M. O'Connor, J.U. Adams, J. Fairman, Essentials of Cell Biology, NPG Education, Cambridge, MA, 2010.
[16] A. Dhar, K. Girdhar, D. Singh, H. Gelman, S. Ebbinghaus, M. Gruebele, Protein stability and folding kinetics in the nucleus and endoplasmic reticulum of eucaryotic cells, Biophys. J . 101 (2011) 421–430.
[17] W.B. Monteith, G.J. Pielak, Residue level quantification of protein stability in living cells, PNAS 111 (2014) 11335–11340.
[18] Y. Wang, M. Sarkar, A.E. Smith, A.S. Krois, G.J. Pielak, Macromolecular crowding and protein stability, J. Am. Chem. Soc. 134 (2012) 16614–16618.
[19] A.P. Schlesinger, Y. Wang, X. Tadeo, O. Millet, G.J. Pielak, Macromolecular crowding fails to fold a globular protein in cells, J. Am. Chem. Soc. 133 (2011) 8082–8085.

[20] D. Davidi, E. Noor, W. Liebermeister, A. Bar-Even, A. Flamholz, K. Tummler, U. Barenholz, M. Goldenfeld, T. Shlomi, R. Milo, Global characterization of in vivo enzyme catalytic rates and their correspondence to in vitro kcat measurements, Proc. Natl. Acad. Sci. 113 (2016) 3401–3406.
[21] H.S. McHaourab, M.A. Lietzow, K. Hideg, W.L. Hubbell, Motion of spin-labeled side chains in T4 lysozyme. Correlation with protein structure and dynamics, Biochemistry 35 (1996) 7692–7704.
[22] L.J. Berliner, J. Grunwald, H.O. Hankovszky, K. Hideg, A novel reversible thiol-specific spin label: papain active site labeling and inhibition, Anal. Biochem. 119 (1982) 450–455.
[23] A.P. Todd, J. Cong, F. Levinthal, C. Levinthal, W.L. Hubell, Site-directed mutagenesis of colicin E1 provides specific attachment sites for spin labels whose spectra are sensitive to local conformation, Proteins: Structure, Function, Bioinf. 6 (1989) 294–305.
[24] I. Krstić, R. Hänsel, O. Romainczyk, J.W. Engels, V. Dötsch, T.F. Prisner, Long-range distance measurements on nucleic acids in cells by pulsed EPR spectroscopy, Angew. Chem. Int. Ed. 50 (2011) 5070–5074.
[25] M. Azarkh, O. Okle, P. Eyring, D.R. Dietrich, M. Drescher, Evaluation of spin labels for in-cell EPR by analysis of nitroxide reduction in cell extract of Xenopus laevis oocytes, J. Magn. Reson. 212 (2011) 450–454.
[26] B. Joseph, A. Sikora, D.S. Cafiso, Ligand induced conformational changes of a membrane transporter in E. coli cells observed with DEER/PELDOR, J. Am. Chem. Soc. 138 (2016) 1844–1847.
[27] A.A. Bobko, I.A. Kirilyuk, I.A. Grigor'ev, J.L. Zweier, V.V. Khramtsov, Reversible reduction of nitroxides to hydroxylamines: roles for ascorbate and glutathione, Free Radical Biol. Med. 42 (2007) 404–412.
[28] A. Martorana, G. Bellapadrona, A. Feintuch, E. Di Gregorio, S. Aime, D. Goldfarb, Probing protein conformation in cells by EPR distance measurements using Gd3+ spin labeling, J. Am. Chem. Soc. 136 (2014) 13458–13465.
[29] M. Qi, A. Groß, G. Jeschke, A. Godt, M. Drescher, Gd(III)-PyMTA label is suitable for in-cell EPR, J. Am. Chem. Soc. 136 (2014) 15366–15378.
[30] F.C. Mascalic, H.Y.V. Ching, R.M. Rasia, S. Un, L.C. Tabares, Using genetically encodable self-assembling GdIII spin labels to make in-cell nanometric distance measurements, Angew. Chem. Int. Ed. 55 (2016) 11041–11043.
[31] J.J. Jassoy, A. Berndhäuser, F. Duthie, S.P. Kühn, G. Hagelueken, O. Schiemann, Versatile trityl spin labels for nanometer distance measurements on biomolecules in vitro and within cells, Angew. Chem. Int. Ed. 56 (2017) 177–181.
[32] A.P. Jagtap, I. Krstić, N.C. Kunjir, R. Hänsel, T.F. Prisner, S.T. Sigurdsson, Sterically shielded spin labels for in-cell EPR spectroscopy: analysis of stability in reducing environment, Free Radical Res. 49 (2015) 78–85.
[33] A.A. Kuzhelev, D.V. Trukhin, O.A. Krumkacheva, R.K. Strizhakov, O.Y. Rogozhnikova, T.I. Troitskaya, M.V. Fedin, V.M. Tormyshev, E.G. Bagryanskaya, Room-temperature electron spin relaxation of triarylmethyl radicals at the X- and Q-bands, J. Phys. Chem. B 119 (2015) 13630–13640.
[34] M.J. Lawless, A. Shimshi, T.F. Cunningham, M.N. Kinde, P. Tang, S. Saxena, Analysis of nitroxide-based distance measurements in cell extracts and in cells by pulsed ESR spectroscopy, ChemPhysChem 18 (2017) 1653–1660.
[35] P. Wipf, J. Xiao, J. Jiang, N.A. Belikova, V.A. Tyurin, M.P. Fink, V.E. Kagan, Mitochondrial targeting of selective electron scavengers: synthesis and biological analysis of Hemigramicidin–TEMPO conjugates, J. Am. Chem. Soc. 127 (2005) 12460–12461.
[36] U.S. Mehrotra, M.C. Agrawal, S.P. Mushran, Kinetics of the reduction of hexacyanoferrate(III) by ascorbic acid, J. Phys. Chem. 73 (1969) 1996–1999.
[37] R. Igarashi, T. Sakai, H. Hara, T. Tenno, T. Tanaka, H. Tochio, M. Shirakawa, Distance determination in proteins inside xenopus laevis oocytes by double electron–electron resonance experiments, J. Am. Chem. Soc. 132 (2010) 8228–8229.
[38] P. Roser, M.J. Schmidt, M. Drescher, D. Summerer, Site-directed spin labeling of proteins for distance measurements in vitro and in cells, Org. Biomol. Chem. 14 (2016) 5468–5476.
[39] J. Cattani, V. Subramaniam, M. Drescher, Room-temperature in-cell EPR spectroscopy: alpha-Synuclein disease variants remain intrinsically disordered in the cell, PCCP 19 (2017) 18147–18151.
[40] S.A. Mendanha, J.L.V. Anjos, A.H.M. Silva, A. Alonso, Electron paramagnetic resonance study of lipid and protein membrane components of erythrocytes oxidized with hydrogen peroxide, Braz. J. Med. Biol. Res. 45 (2012) 473–481.
[41] G. Karthikeyan, A. Bonucci, G. Casano, G. Gerbaud, S. Abel, V. Thomé, L. Kodjabachian, A. Magalon, B. Guigliarelli, V. Belle, O. Ouari, E. Mileo, A bioresistant nitroxide spin label for in-cell EPR spectroscopy: in vitro and in oocytes protein structural dynamics studies, Angew. Chem. Int. Ed. 57 (2018) 1366–1370.
[42] T.F. Cunningham, M.S. McGoff, I. Sengupta, C.P. Jaroniec, W.S. Horne, S. Saxena, High-resolution structure of a protein spin-label in a solvent-exposed β-sheet and comparison with DEER spectroscopy, Biochemistry 51 (2012) 6350–6359.
[43] T.F. Cunningham, S. Pornsuwan, W.S. Horne, S. Saxena, Rotameric preferences of a protein spin label at edge-strand β-sheet sites, Protein Sci. 25 (2016) 1049–1060.
[44] G. Jeschke, V. Chechik, P. Ionita, A. Godt, H. Zimmermann, J. Banham, C.R. Timmel, D. Hilger, H. Jung, DeerAnalysis2006—a comprehensive software package for analyzing pulsed ELDOR data, Appl. Magn. Reson. 30 (2006) 473–498.
[45] C. Kroll, A. Langner, H.-H. Borchert, Nitroxide metabolism in the human keratinocyte cell line HaCaT11Dedicated to Prof. Dr. G. Heinisch, Innsbruck, Austria, on the occasion of his 60th birthday, Free Radical Biol. Med. 26 (1999) 850–857.
[46] H.M. Swartz, M. Sentjurc, P.D. Morse, Cellular metabolism of water-soluble nitroxides: effect on rate of reduction of cell/nitroxide ratio, oxygen concentrations and permeability of nitroxides, Biochim. Biophys. Acta (BBA) – Mol. Cell Res. 888 (1986) 82–90.
[47] S. Ghosh, M.J. Lawless, G.S. Rule, S. Saxena, The Cu2+-nitrilotriacetic acid complex improves loading of α-helical double histidine site for precise distance measurements by pulsed ESR, J. Magn. Reson. 286 (2018) 163–171.
[48] M.J. Lawless, S. Ghosh, T.F. Cunningham, A. Shimshi, S. Saxena, On the use of the Cu2+–iminodiacetic acid complex for double histidine based distance measurements by pulsed ESR, PCCP 19 (2017) 20959–20967.
[49] Z. Yang, M. Ji, S. Saxena, Practical aspects of copper ion-based double electron electron resonance distance measurements, Appl. Magn. Reson. 39 (2010) 487–500.
[50] S.G. Rhee, H.Z. Chae, K. Kim, Peroxiredoxins: a historical overview and speculative preview of novel mechanisms and emerging concepts in cell signaling, Free Radical Biol. Med. 38 (2005) 1543–1552.
[51] D.M. Ziegler, Role of reversible oxidation-reduction of enzyme thiols-disulfides in metabolic regulation, Annu. Rev. Biochem. 54 (1985) 305–329.
[52] B. Joseph, A. Sikora, E. Bordignon, G. Jeschke, D.S. Cafiso, T.F. Prisner, Distance measurement on an endogenous membrane transporter in E. coli cells and native membranes using epr spectroscopy, Angew. Chem. (Int. English) 54 (2015) 6196–6199.